Effect of N_2^* and N on GaN nanocolumns grown on Si(111) by molecular beam epitaxy

A. Debnath, J. S. Gandhi, M. Kesaria, R. Pillai, D. Starikov, and A. Bensaoula

Citation: Journal of Applied Physics **119**, 104302 (2016); doi: 10.1063/1.4943179
View online: https://doi.org/10.1063/1.4943179
View Table of Contents: http://aip.scitation.org/toc/jap/119/10
Published by the American Institute of Physics

JOURNAL OF APPLIED PHYSICS **119**, 104302 (2016)

Effect of N_2^* and N on GaN nanocolumns grown on Si(111) by molecular beam epitaxy

A. Debnath,[1,a)] J. S. Gandhi,[1,2] M. Kesaria,[1] R. Pillai,[2] D. Starikov,[2] and A. Bensaoula[2]
[1]*Department of Physics, SR1 617, University of Houston, Houston, Texas 77204, USA*
[2]*Integrated Micro Sensors, Inc., Houston, Texas 77096, USA*

(Received 20 November 2015; accepted 21 February 2016; published online 9 March 2016)

The self-induced growth of GaN nanocolumns (NCs) on Si_xN_{1-x}/Si (111) is investigated as a function of the ratio of molecular to atomic nitrogen species generated via plasma assisted molecular beam epitaxy. Relative concentrations of the molecular and atomic species are calculated using optical emission spectroscopy. The growth rate (GR), diameter, and density of NCs are found to vary with the molecular to atomic nitrogen species relative abundance ratio within the plasma cavity. With increasing ratio, the GR and diameter of NCs increase while the density of NCs seems to be decreasing. The morphologies and the coalescence of GaN NCs exhibit a trend for molecular/atomic ratios up to 11, beyond which they still change but at a lower rate. The detrimental effect of taperedness of the NCs decreases with increasing molecular/atomic ratios. This is possibly because of reduction in radial growth in NCs due to increase in diffusivity of nitrogen species with increasing ratios. © *2016 AIP Publishing LLC*. [http://dx.doi.org/10.1063/1.4943179]

I. INTRODUCTION

Gallium nitride (GaN) nanocolumns (NCs) are found suitable for low-cost, high-performance wide band gap electronic devices, such as light emitting diodes[1–3] lasers[4,5] and field effect transistor applications.[6] Previous literature reports on the catalyst assisted growth of GaN NCs employed numerous techniques, viz., organometallics vapor phase epitaxy (OMVPE), hydride vapor phase epitaxy (HVPE), metalorganic molecular beam epitaxy (MOMBE), and direct synthesis. In catalyst free MBE, GaN NCs form spontaneously. Though there are several reports on self-induced GaN NC growth by MBE,[7–9] the understanding of structural/morphological evolution of NCs has been challenging. Self-induced NCs have been reported on various substrates, e.g., sapphire[10] and silicon,[11] with or without a starting buffer layer, e.g., AlN[12] and Si_xN_y,[13] and under nitrogen rich conditions without any catalyst. In those reports, the morphologies, density, length, and diameter of NCs were shown to be influenced by growth parameters such as Ga flux,[14] substrate type, substrate temperature,[15] buffer layers,[16] surface energy, and sticking coefficients.[17] However, there exists a discrepancy between the reported growth conditions and the resulting NC morphologies. One aspect that has been understudied, especially in the plasma assisted GaN NC growths, is the effect of nitrogen species. Due to the multiple states and concentrations of the available excited species, it has been difficult to quantify and correlate their role with the morphologies of the resulting NCs. As such, a comprehensive GaN NC growth model encompassing the effect of species remains to be desired. Out of few reported studies on the effect of species, Bertness *et al.* reported an increase in growth rate (GR) with increasing molecular N_2 species for GaN NCs grown on an AlN buffer layer on Si(111) and stressed on the necessity of an AlN buffer layer and excess of N atoms on the nucleation of GaN NCs.[18]

Optical Emission Spectroscopy (OES) is generally used to characterize the emission spectra from the RF nitrogen plasma source. OES gives information about which nitrogen species (N and N_2^*) are dominant in the plasma chamber and how their relative abundance varies with power and flow rate. But the actual concentration of species or their ratio reaching the substrate surface is not necessary the same as that measured by OES. The relative abundance of the various species inside and outside of the plasma cavity is determined by the source geometry and the specifics of the Pyrolitic Boron Nitride (PBN) exit aperture design as well as the species charge, energy and, relaxation and recombination times. Ptak *et al.*[19] showed that the growth rate of GaN thin film depends on both atomic N and metastable N_2^* flux. Using OES, Iliopoulos *et al.*[20] and Kikuchi *et al.*[21] have correlated the effect of the relative concentration of N and N_2^* with GaN thin film GR. Carrere *et al.*[22] further demonstrated this for dilute nitrides. Furthermore, by line-of-sight threshold ionization mass spectrometry, Agarwal *et al.*[23] showed the best way to determine the absolute densities of N and N_2^* at the substrate plane in an inductively coupled N_2 plasma. Similarly, Meyers *et al.*[24] used the source in a direct line of sight of a quadrupole mass spectrometer (QMS) and measured the effect of atomic and metastable nitrogen flux on the GR and electrical properties of GaN thin film. In a nitrogen plasma, the dissociation degree (D) can be estimated by QMS.[25] By OES, Vaudo *et al.*[26] showed a more direct measurement of the dissociation degree and proposed the estimation of D in nitrogen plasmas based on the atomic to molecular ratios. Based on the combined OES and QMS experiments, McCullogh *et al.*[27,28] found a linear relationship between the intensity of the atomic nitrogen line 746.8 nm and the intensity of 4–2 molecular band (750.4 nm) of the first positive system and the quantity D/(1-D). Also, Cho *et al.*[29] conducted a comparative study

a)Author to whom correspondence should be addressed. Electronic mail: ananyadebnth@gmail.com.

between ECR and RF plasma sources using QMS and OES and found that the RF sources generate a higher atomic than molecular nitrogen species density and are more favorable to getting lower state molecular and atomic nitrogen species and a good correlation between the OES (inside the cavity) and QMS (near the substrate) intensities. Thus, the OES done inside the plasma cavity is a good qualitative measurement of the relative abundance of N species reaching the substrate surface.

In this work, reflection high energy electron diffraction (RHEED) and field emission scanning electron microscopy (FESEM) are employed for surface structure, plan-view, and cross-sectional imaging of GaN NCs. OES is used to characterize the emission spectra from the RF nitrogen plasma source in order to calculate (C_{mol}/C_{at}) ratio of nitrogen species for the entire range of varying power and flow rate of RF nitrogen plasma source. GaN NC morphologies have been compared in the following scenarios: (a) modulating the concentration of molecular species (C_{mol}) while keeping the atomic species concentration (C_{at}) constant, (b) modulating the concentration of atomic species (C_{at}) while keeping the molecular species concentration (C_{mol}) constant, and (c) identifying the effect of the molecular/atomic ratio (C_{mol}/C_{at}) of species on the morphologies. Thus, the effect of modulating the molecular and atomic nitrogen species on the morphology, length, size, and density of GaN NC on Si_xN_y/Si substrates is studied.

II. EXPERIMENTAL

The GaN NCs are grown in a conventional custom made MBE system outfitted with a Knudsen cell for gallium and a Veeco Uni bulb RF nitrogen plasma source for N. The Si (111) wafers are prepared for growth by degreasing in trichloroethylene, acetone, and methanol, 5 min each, followed by 1 min etch in a HF:CH3OH (1:9) mixture by volume, followed by rinsing in deionized water, and blown dry with nitrogen. After chemical cleaning, the substrate is degassed in a preparation chamber at ~125 °C for 1 h and then deoxidized at 830 °C in the growth chamber, as confirmed by observation of a 7 × 7 RHEED reconstruction pattern. A thin silicon nitride layer is formed on the Si (111) wafer by exposing the surface to a nitrogen plasma flux for 35 s for nitridation. The Ga beam equivalent pressure (BEP) is kept at 4×10^{-7} Torr, the substrate temperature is kept constant at 742 °C, and growth time of 2 h for five samples numbered 1, 2, 3, 4, and 5. The BEP is measured using an ion gauge, while a pyrometer is used to monitor the growth temperature as a blackbody radiation emitted from the Si substrate. The reported RF power is the forward-going power into the plasma which is varied from 375 to 450 W, whereas reflected power around 0 W is kept same for all samples. Nitrogen flow rate in standard cubic centimeter per minute (sccm) unit is controlled and measured by a mass flow controller. The uncertainty in nitrogen flow rate is typically ±0.01 sccm and in BEP is $\pm 0.1 \times 10^{-5}$ Torr. The power range of 250 W to 500 W and the flow rates of 0.50 sccm to 4.00 sccm are employed. Once the entire range was defined, then the spectra for each possible individual condition of power and flow rates were studied and the selection of the 5 specific conditions discussed in this work is summarized in Table I. *In-situ* RHEED images are taken every minute for the first 20 min and then every 10 min (but only relevant images are included here). High resolution FESEM is employed for cross-sectional and plan-view imaging, with a line resolution of 5 nm. Height of the nanocolumns is measured from cross-sectional imaging of cleaved pieces.

TABLE I. The growth conditions for five GaN NC samples.

Sample	Nitrogen plasma power (W)	Nitrogen flow rate (sccm)	V/III ratio	C_{mol}/C_{at} ratio
1	450	0.50	23	9.6
2	450	2.00	97	11.2
3	450	2.80	142	14.1
4	430	0.95	45	10.3
5	375	2.10	105	15.6

The optical emission of N plasma is collected by a lens mounted at the base of a view port in line of sight of the plasma discharge. A fiber optics cable is connected between the lens and a diffraction grating with the resulting signal amplified by a photomultiplier tube. The absolute intensities are sensitive to the lens mounting, and to maintain consistency all samples are grown consecutively without disturbing the lens mount. Otherwise, careful realignment of the optics to obtain similar OES signals for a set power and flow conditions is performed. Furthermore, the optical spectra are captured before, during, and at the end of each growth to confirm the stability of the plasma conditions. In an RF nitrogen plasma source, the relative abundance of the nitrogen species can be varied through control of two parameters: plasma power and nitrogen flow rate. The plasma composition was investigated by OES.[20] Fig. 1 corresponds to emission spectra captured within the 500–880 nm range for an RF power of 450 W and N_2 flow rate of 2.0 sccm. The broad band emission (570–680 nm) corresponds to the first positive series of excited molecular N_2^* arising from $B^3\pi_g$ to $A^3\Sigma_u$ transitions.[30] The peaks centered at 744.6 nm, 821.3 nm, and 865.8 nm are the emission from multiplets of atomic nitrogen N.[30] The concentration of molecular N_2^* species (C_{mol}) is calculated using the total area under the curve

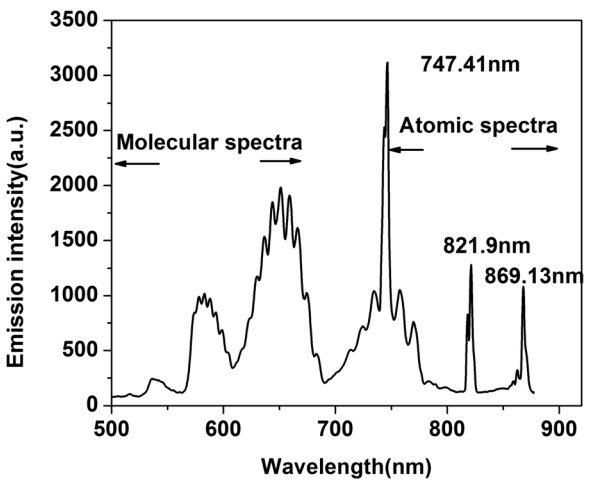

FIG. 1. Representative emission spectra of nitrogen plasma acquired at 450 W RF power and 2.00 sccm nitrogen flow rate.

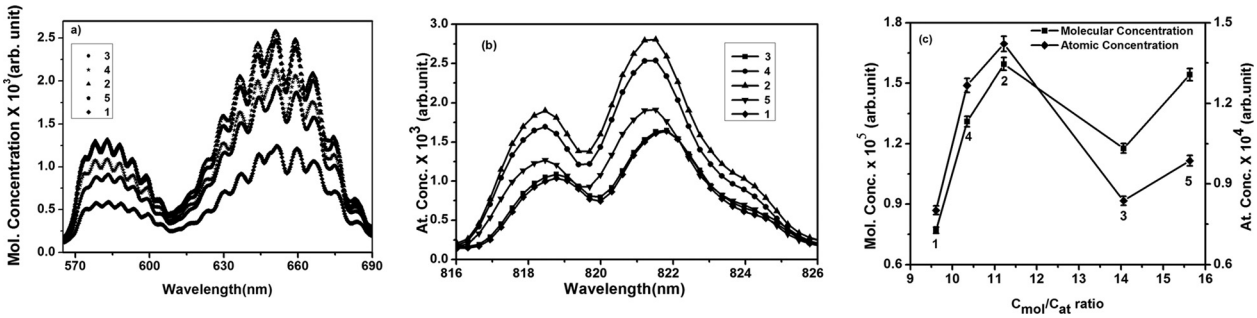

FIG. 2. Optical emission for different nitrogen plasma conditions for spectral regions representing (a) excited molecular N_2, (b) atomic N lines for samples 1, 2, 3, 4, and 5, and (c) molecular and atomic concentrations (with samples 1, 4, 2, 3, and 5) plotted as a function of C_{mol}/C_{at} ratio. The insets in Figures 2(a) and 2(b) represent the sample number.

within the spectral range (562–691 nm) and the concentration of atomic N species (C_{at}) is calculated by taking the area under the spectral line (816–826 nm). C_{mol}/C_{at} ratio is then calculated as a function of power and flow rate. It is to be noted that the plasma source was characterized over the entire range of power and flow rates that would yield bright and stable plasma conditions. In order to do background correction, the nitrogen emission spectra of the blank substrate were obtained under experimental condition, both the blank and experimental spectra were baseline corrected, and then blank spectra were subtracted from the experimental emission spectra using Origin software. After calculating the area under the curve, the C_{mol}/C_{at} ratios are: for sample 1 (9.6), sample 4 (10.3), sample 2 (11.2), sample 3 (14.1), and sample 5 (15.6).

III. RESULT AND DISCUSSION

Figs. 2(a) and 2(b) represent the respective molecular N_2^* bands and atomic N lines for samples 1, 2, 3, 4, and 5. Sample 2 yielded highest total concentration of molecular N_2^* species followed by 5, 4, 3, and 1 (Fig. 2(a)). In Fig. 2(b), the concentration of atomic N peak in OES for samples $2 > 4 > 5 > 3 > 1$ is shown. Fig. 2(c) shows the variation of molecular and atomic nitrogen species concentration as a function of the ratio C_{mol}/C_{at} with sample numbers corresponding to their ratios. The total concentration of the species is calculated by adding the total concentration of molecular species over 562–691 nm range and atomic species over 816–826 nm range. The total intensities (measured in arbitrary units) are 85 064, 173 698, 126 081, 143 724, and 160 653, for samples 1, 2, 3, 4, and 5, respectively. It is to be noted that various powers and flow rates were specifically selected to modulate the ratio of the atomic to molecular nitrogen species. As such, we can see that three plasma conditions were utilized with nearly identical powers, while the other two conditions utilized with near identical flow rates, yet the resulting concentrations were different. Hence, the focus of this work is to study the trend in GaN NC morphology as a function of C_{mol}/C_{at} ratio.

Prior to GaN growth, the oxide free Si (111) surface is confirmed by observing a 7×7 RHEED reconstruction (Fig. 3(a)) after a high temperature sample degassing. RHEED patterns (Fig. 3(b)) with a bright background indicate that the silicon nitride layer is a mixture of crystalline and amorphous phases.[31] At 742 °C, the nitride layer is exposed to the Ga flux and nitrogen species. As soon as GaN growth begins, the RHEED intensity diminishes and no RHEED reconstructions are observed over a period of 5 to 16 min, called the incubation time.[8] The incubation time is the time required for the starting of the NC growth. The incubation time for the NC samples varies from 5 to 16 min. For

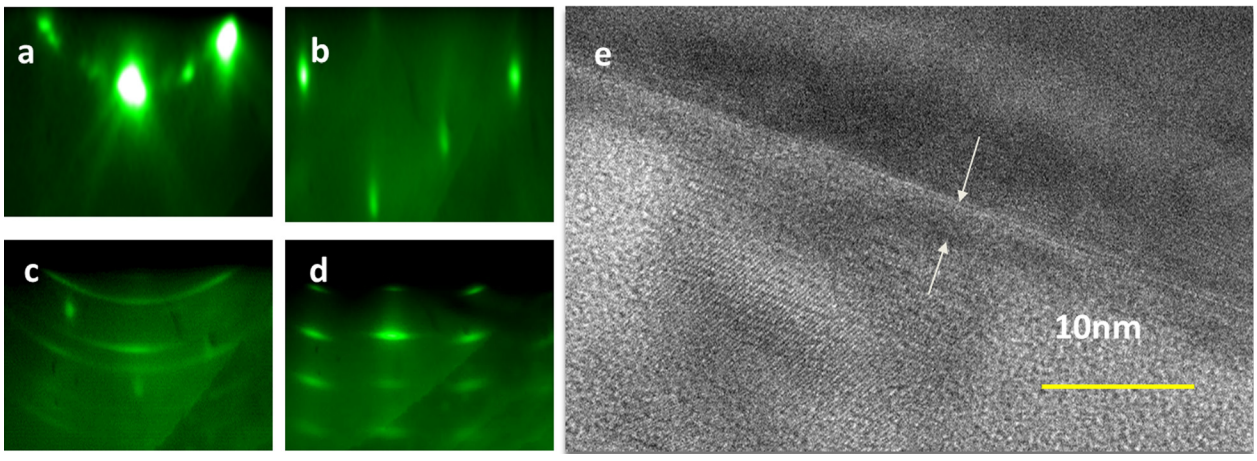

FIG. 3. Four typical RHEED images captured during NC growth. (a) 7×7 reconstruction of bare Si prior to nitridation, (b) Si_xN_y layer after 35 s of nitridation, (c) GaN NC nucleation on Si_xN_y layer, (d) GaN NCs at the end of growth, and (e) TEM image of silicon nitride layer (shown by the arrows) on Si (111) for the NCs. Marker bar of the image is 10 nm.

samples 1, 2, and 3, the N_2 plasma power is kept constant at 450 W and flowrate is changed to 0.5, 2.0, and 2.8 sccm, respectively. The incubation time is found to be 14, 9, and 5 min. With increasing flowrate, the active metastable N_2^* population increases which raises the island nucleation rate and hence decreases the incubation time as per the island nucleation theory.[8] With increasing C_{mol}/C_{at} nitrogen ratio, a decrement in the incubation time for the GaN NC samples can be observed. All the NC samples are grown effectively for 2 h excluding the incubation time. At the end of this incubation period, RHEED patterns transform to a broken rings plus spots pattern suggesting nucleation of randomly oriented crystalline GaN NCs (Fig. 3(c)). With continued growth, the long ring like structures transform into a RHEED pattern with elongated spots which indicates growth of wurtzite (WZ) 3D GaN NCs as seen from the [11$\bar{2}$ 0] azimuthal sample direction (Fig. 3(d)).[32] The broadening in RHEED images implies a slight spread in the orientation of the GaN NCs with respect to the Si (111) substrate.[33] A thin silicon nitride layer ~2.0–3.0 nm is formed at high temperature on the Si (111) substrate *via* nitridation by exposing the sample to the plasma for 35 s (Fig. 3(e)).

Fig. 4 identifies samples for each set of cross sectional and plan view images. The cross sectional images show that the columns are well separated and the plan views show that NCs have cross-sections which are either regular hexagons or six-sided polygons. In the plan FESEM views, Figs. 4(b), 4(d), 4(f), 4(h), and 4(j), the top facet of NCs is parallel to the substrate along c-plane (0001). In some cases, the NCs cross-section appears as a six sided irregular polygon which might be due to coalescence of adjacent NCs. The observed bending of NCs, as seen in plan view images, is a result of electrostatic charging or damage caused due to sample cleavage. The GR of the NCs is calculated from the cross sectional SEM images (Figs. 4(a), 4(c), 4(e), 4(g), and 4(i)). The length of NCs has been determined by using cross sectional FESEM image. The length has been measured manually as well as by using the ImageJ software. The GR has been determined by dividing the length by total growth time. The NCs diameter and density were determined from the plan-view FESEM images (Figs. 4(b), 4(d), 4(f), 4(h), and 4(j)) using the ImageJ software. To determine the diameter and density, at first, a low magnification was chosen and the whole image was divided into few segments. The edges of the cluster were detected by adjusting the threshold, and average surface area of the cluster was determined. Average surface area of single NC was determined by recognizing the NC in the cluster. Density was determined by dividing the cluster surface area by NC mean surface area.[34] The result obtained is averaged over few iterations. The average NC diameter thus obtained is different than the cluster diameter. The average growth rate, diameter, and density of nanocolumns samples are displayed in Fig. 5.

The NCs are smaller in diameter and shorter in length for sample 1 (Figs. 4(b) and 4(a)) with lowest C_{mol}/C_{at} ratio of 9.6 and grow larger in diameter and length as the ratio increases to 10.3 and 11.2 for samples 4 and 2, respectively. Afterwards, the GR gets saturated even if the ratio increases beyond 11.2 but the diameter gradually increases with

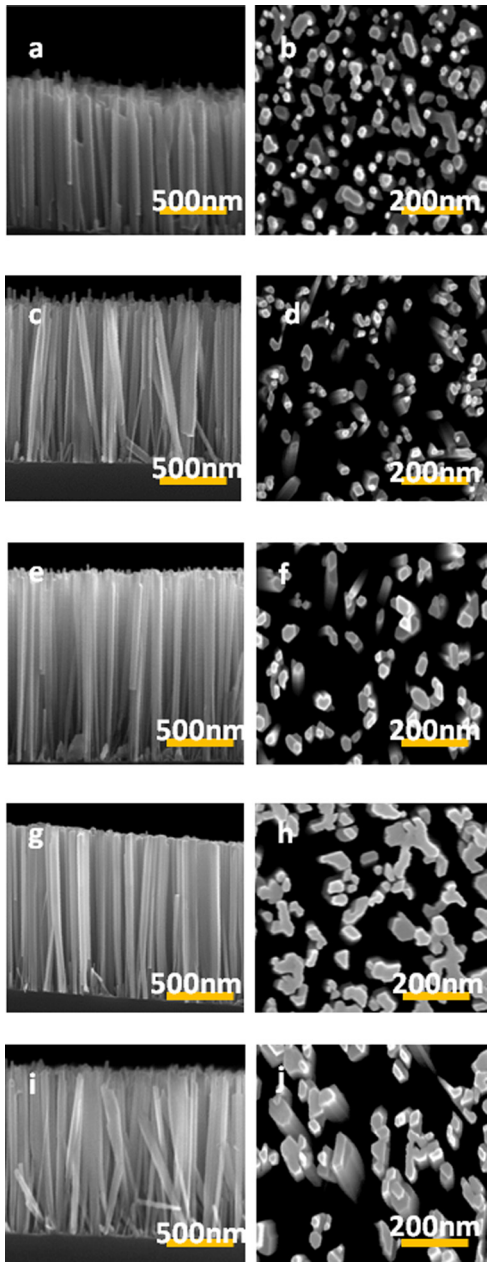

FIG. 4. (a), (c), (e), (g), and (i) represent cross sectional SEM images of samples 1, 4, 2, 3, and 5, respectively, while (b), (d), (f), (h), and (j) represent the plan view of the same. Marker bar for cross sectional images is 500 nm and that for plan view images is 200 nm.

increasing ratio. The average GR and diameter of the NCs for these samples vary from 4.8 to 12.8 nm/min and from 45 to 77 nm, respectively, depending on the ratio of nitrogen species C_{mol}/C_{at}. The density of the NCs varies from 188 to 45 μm^{-2} as the ratio changes from 9.6 to 15.6. Also with increasing ratio, the NCs are found to be more coalesced in samples 3 and 5 as can be seen in Figs. 4(h) and 4(j), respectively. The degree of coalescence of the NCs is determined by the following formula: $\alpha_{coalescence} = 1 - (\rho_{cluster}/\rho_{NC})$. When coalescence is small, the cluster density approaches NC density and is given by a very small fractional value. As coalescence increases, the cluster density is much smaller than the NC density, giving rise to a bigger fractional value.

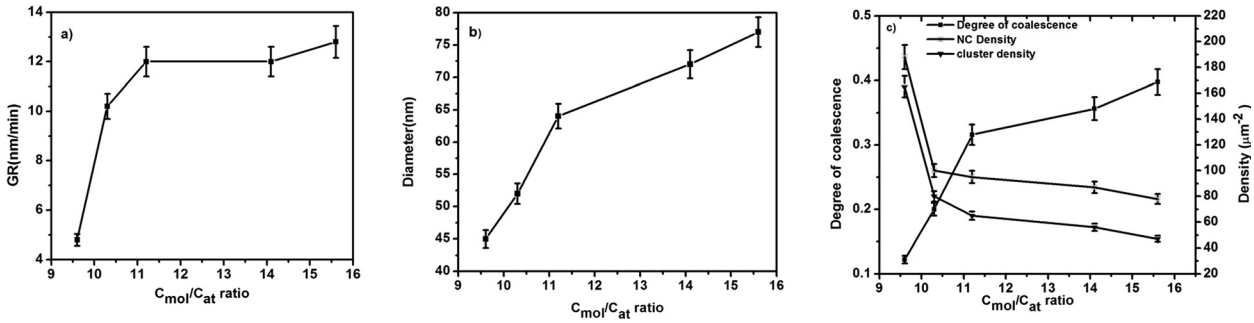

FIG. 5. The diagrams represent plot for (a) GR, (b) diameter, and (c) NC density, cluster density, and degree of coalescence of GaN NCs as a function of C_{mol}/C_{at} ratio of nitrogen species.

The variation of the degree of coalescence with C_{mol}/C_{at} ratio (Fig. 5(c)) shows that the NCs experience a rapid increase in radial growth rate with increasing C_{mol}/C_{at} ratio till 11.2, and then the radial growth rate slowly increases causing coalescence to saturate as C_{mol}/C_{at} ratio increases. This explains why the diameter increment is initially abrupt and then gradual as a function of C_{mol}/C_{at} ratio.

For MBE grown self-induced GaN NCs, the factors governing the NC nucleation and growth are still under debate. Bertness *et al.*[18] discussed how the molecular and atomic nitrogen species affect the GR and nucleation of GaN NCs on AlN/Si(111). In their work, the GR of NCs increased with higher excited molecular N_2^* species, which were selected by increasing the nitrogen gas flow (with no significant effect of plasma power), whereas the nucleation density of NCs increased with increasing concentration of the atomic nitrogen species. Our experimental results show that samples 2 and 5 grown with almost the same nitrogen flow rates but different nitrogen plasma powers yielded near identical molecular spectral concentration (see Figs. 2(a) and 2(c)). The NCs GR for these two samples is nearly identical (see Fig. 5(a)), which supports the findings in Ref. 18. We have observed that lowering the RF power for the N_2 plasma source from 450 W (sample 2) to 375 W (sample 5) has increased the diameter of the NCs as they grow (Fig. 5(b)). The lower RF power has reduced atomic N flux and increased the Ga migration length for lateral growth. Two other samples, 1 and 3, are grown with the same nitrogen plasma power but different nitrogen flow rates which yielded the same atomic line species concentrations (see Figs. 2(b) and 2(c)). Under a high nitrogen flow rate (sample 3), GaN nucleation density is high. For a low nitrogen flow rate (sample 1), GaN nucleation density is low at the initial stage of growth.[10] For a low nucleation density, initial GaN islands are widely separated with more nucleates forming due to the small nitrogen migration length. This induces size fluctuation and height randomness as is evident from Fig. 4(a)). Hence, as seen in sample 1, the NC density increases abruptly with time ultimately resulting in shadowing effect and a lower GR. The consequence of a higher nucleation density is usually coalescence of neighbouring NCs. This is seen in sample 3 where, with increasing growth time, the close proximity of the islands leads to increased coalescence and a drop in the final NC density (see Fig. 5(c)). This could be the reason behind the measured drop in NC density with increased flow rate.

In addition, for samples 1, 2, and 3, the nitrogen plasma conditions are such that the concentration of excited molecular N_2^* species varies in the following order: sample 2 > sample 3 > sample 1 (see Figs. 2(a) and 2(c)). It is evident from Fig. 5(a) that the GR of GaN NCs increases with higher excited molecular N_2^* species (which supports Ref. 18) up to a certain point and then GR remains the same (for samples 2 and 3). Also, the change in RF power for samples 2 and 5 changes the concentration of the atomic N species, which varies as follows: sample 2 > sample 5 (see Figs. 2(b) and 2(c)). So, the nucleation density of GaN NCs is higher in sample 2 than in 5 as per Bertness *et al.*[18] and so is the NC density as is evident from Fig. 5(c)) though there is coalescence to some extent in both samples. But when the sample 4 is included in the analysis, the change in NCs GR, diameter, and density can be explained using the C_{mol}/C_{at} ratio instead.

The changes in GR, diameter, and density of the columns with C_{mol}/C_{at} nitrogen ratio are shown in Fig. 5. We can observe from Fig. 5(a) that the GaN NCs GR has two distinct regions: GR increases rapidly as the C_{mol}/C_{at} ratio increases from 9.6 to 11.2, beyond which it stays constant. The NC diameter increases monotonically from 45 to 77 nm for C_{mol}/C_{at} ratio up to 11.2 beyond which it still increases but at a lower rate up to 15.6 (Fig. 5(b)). The NC density, the cluster density, and the degree of coalescence are plotted in Fig. 5(c) as a function of the nitrogen C_{mol}/C_{at} ratio. The NC density (cluster density) evolution follows two steps: The density abruptly drops from 188 to 100 μm^{-2} (165 to 80 μm^{-2}) when the C_{mol}/C_{at} ratio increases from 9.6 to 10.3 and then slowly decreases to 75 μm^{-2} (47 μm^{-2}) with increasing C_{mol}/C_{at} ratio. The degree of coalescence initially increases till a C_{mol}/C_{at} ratio of 11.2, beyond which the increase rate is lower until it reaches a final value of 0.4. In Fig. 5(c), the NC density decreases drastically as C_{mol}/C_{at} increases from 9.6 to 10.3 with a slower change with continued increase in the ratio. Nevertheless, the C_{mol}/C_{at} parameter seems to be vital in any attempt to model the GaN NC growth process, as it is clear that the density of the individual N species alone is not sufficient to understand the growth mechanism. From the evolution of GR with C_{mol}/C_{at} ratio (Fig. 5(a)), it can be assumed that initially the sidewall diffusion of active N_2^* increases (sample 4, with C_{mol}/C_{at} ratio 10.3) with increasing ratio and then the diffusivity of N_2^* saturates at a higher C_{mol}/C_{at} ratio (sample 5 with C_{mol}/C_{at} ratio 15.6). Diameter evolution

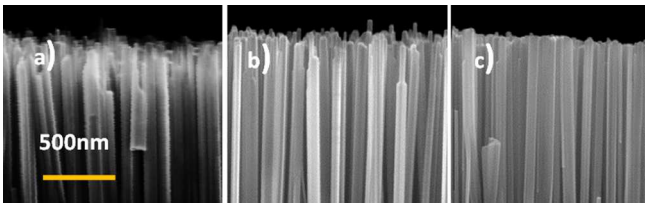

FIG. 6. Images (a), (b), and (c) represent cross sectional images of GaN NC with C_{mol}/C_{at} ratio of 9.6, 11.2, and 14.1, respectively. Images show tapering of NCs reduce with increasing C_{mol}/C_{at} ratio.

(Fig. 5(b)) of GaN NCs from sample 4 to 5 is possibly because of the increasing diffusion of active metastable N_2^* on the NC top with increasing ratio. Thus, the nature of increase of the diffusion length of active metastable N_2^* is also different on the two planes, which results in a plateau in NC GR and a gradual increase in NC diameter with increasing C_{mol}/C_{at} ratio.

Close inspection of the GaN NC samples shows that as the C_{mol}/C_{at} ratio increases the tapering of NCs decreases (Fig. 6). The possible reason may be the increasing diffusivity of active metastable N_2^* with increasing ratio. The plot of coalescence as a function of C_{mol}/C_{at} ratio also shows that the radial growth rate of NCs tends to saturate beyond a C_{mol}/C_{at} ratio of 11.2. The quantity GR $\times$ diameter $\times$ density, which is equivalent to the total amount of material deposited, shows a gradual rise in the beginning followed by saturation as the ratio increases. This is probably the result of limited increase in diffusion of N species on m- and c-planes at the higher ratios. Overall, the above results show that while the V/III ratio is usually the main control parameter reported during the growth of both 2D and 3D thin GaN layers, the relative abundance of the various active species, independent of the RF source flow rate and power, is more critical with respect to the morphology, GR, and density in the NCs growth regime. Thus, the relevance of using the C_{mol}/C_{at} ratio as an additional parameter in understanding the mechanism of GaN NCs by MBE is established.

IV. CONCLUSION

GaN NCs are spontaneously grown on Si_xN_{1-x}/Si (111) by RFMBE and their morphologies are characterized as a function of the ratio of molecular to atomic intensities obtained by varying the RF plasma source power and N_2 flow rate. GR, diameter, and density of GaN NCs exhibited significant changes with initial increase in C_{mol}/C_{at} nitrogen ratio, but the changes becoming more gradual for larger values. The incubation time decreases at a higher ratio, possibly because of the higher nucleation rate. The changes in GR and diameter with C_{mol}/C_{at} nitrogen ratio are due to the possible increase in diffusion of active metastable N_2^* over m- and c-planes with increasing C_{mol}/C_{at} ratio, but the rate of increase in diffusivity slows down because of higher concentration of nitrogen species at these higher ratios. This results in decrease in radial growth rate at a higher C_{mol}/C_{at} nitrogen ratio suppressing taperedness in NCs and giving rise to uniformity in NC diameter.

ACKNOWLEDGMENTS

We would like to thank Mr. Alan Price's technical support during this project and acknowledge partial funding from the NASA SBIR program to Integrated Micro Sensors, Inc.

[1]A. Kikuchi, M. Kawai, M. Tada, and K. Kishino, "InGaN/GaN multiple quantum disk nanocolumn light-emitting diodes grown on (111) Si substrate," Jpn. J. Appl. Phys., Part 1 **43**, L1524–L1526 (2004).
[2]H.-M. Kim, Y. H. Cho, H. Lee, S. I. Kim, S. R. Ryu, D. Y. Kim, T. W. Kang, and K. S. Chung, "High-brightness light emitting diodes using dislocation-free indium gallium nitride/gallium nitride multiquantum-well nanorod arrays," Nano Lett. **4**, 1059–1062 (2004).
[3]Z. Zhong, F. Qian, D. Wang, and C. M. Lieber, "Synthesis of p-type gallium nitride nanowires for electronic and photonic nanodevices," Nano Lett. **3**, 343–346 (2003).
[4]J. C. Johnson, H. J. Choi, K. P. Knutsen, R. D. Schaller, P. Yang, and R. J. Saykally, "Single gallium nitride nanowire lasers," Nat. Mater. **1**, 106–110 (2002).
[5]J. Ristic′, E. Calleja, S. Fernandez-Garrido, A. Trampert, U. Jahn, K. H. Ploog, M. Povoloskyi, and A. Di Carlo, "GaN/AlGaN nanocavities with AlN/GaN Bragg reflectors grown in AlGaN nanocolumns by plasma assisted MBE," Phys. Status Solidi A **202**, 367–371 (2005).
[6]E. Stern, G. G. Cheng, E. Cimpoiasu, R. Klie, S. Guthrie, J. Klemic, I. Kretzschmar, E. Steinlauf, D. Turner-Evans, E. Broomfield, J. Hyland, R. Koudelka, T. Boone, M. Young, A. Sanders, R. Munden, T. Lee, D. Routenberg, and M. A. Reed, "Electrical characterization of single GaN nanowires," Nanotechnology **16**, 2941–2953 (2005).
[7]C. Cheze, L. Geelhaar, A. Trampert, and H. Riechert, "*In situ* investigation of self-induced GaN nanowire nucleation on Si," Appl. Phys. Lett. **97**, 043101 (2010).
[8]V. Consonni, A. Trampert, L. Geelhaar, and H. Riechert, "Physical origin of the incubation time of self-induced GaN nanowires," Appl. Phys. Lett. **99**, 033102 (2011).
[9]M. D. Brubaker, I. Levin, A. V. Davyvov, D. M. Rourke, N. A. Sanford, V. M. Bright, and K. A. Bertness, "Effect of AlN buffer layer properties on the morphology and polarity of GaN nanowires grown by molecular beam epitaxy," J. Appl. Phys. **110**, 053506 (2011).
[10]M. Yoshizawa, A. Kikuchi, M. Mori, N. Fujita, and K. Kishino, "Growth of self-organized GaN nanostructures on Al_2O_3 (0001) by RF-radical source molecular beam epitaxy," Jpn. J. Appl. Phys., Part 1 **36**, L459–L462 (1997).
[11]M. A. Sanchez-Garcia, E. Calleja, E. Monroy, F. J. Sanchez, F. Calle, E. Mũnoz, and R. Beresford, "The effect of the III/V ratio and substrate temperature on the morphology and properties of GaN- and AlN-layers grown by molecular beam epitaxy on Si(111)," J. Cryst. Growth **183**, 23–30 (1998).
[12]V. Consonni, M. Knelangen, L. Geelhaar, A. Trampert, and H. Riechert, "Nucleation mechanisms of epitaxial GaN nanowires: Origin of their self-induced formation and initial radius," Phys. Rev. B **81**, 085310 (2010).
[13]V. Consonni, M. Hanke, M. Knelangen, L. Geelhaar, A. Trampert, and H. Riechert, "Nucleation mechanisms of self-induced GaN nanowires grown on an amorphous interlayer," Phys. Rev. B **83**, 035310 (2011).
[14]S. Fernández-Garrido, J. Grandal, E. Calleja, M. A. Sánchez-García, and D. López-Romero, "A growth diagram for plasma-assisted molecular beam epitaxy of GaN nanocolumns on Si(111)," J. Appl. Phys. **106**, 126102 (2009).
[15]J. Ristic, E. Calleja, S. Ferna′ndez-Garrido, L. Cerutti, A. Trampert, U. Jahn, and K. H. Ploog, "On the mechanisms of spontaneous growth of III-nitride nanocolumns by plasma-assisted molecular beam epitaxy," J. Cryst. Growth **310**, 4035–4045 (2008).
[16]K. A. Bertness, A. Roshko, N. A. Sanford, J. M. Barker, and A. V. Davydov, "Spontaneously grown GaN and AlGaN nanowires," J. Cryst. Growth **287**, 522–527 (2006).
[17]L. Lymperakis and J. Neugebauer, "Large anisotropic adatom kinetics on nonpolar GaN surfaces: Consequences for surface morphologies and nanowire growth," Phys. Rev. B **79**, 241308 (2009).
[18]K. A. Bertness, A. Roshko, L. M. Mansfield, T. E. Harvey, and N. A. Sanford, "Nucleation conditions for catalyst-free GaN nanowires," J. Cryst. Growth **300**, 94–99 (2007).
[19]A. J. Ptak, M. R. Millecchica, T. H. Meyers, K. S. Ziemer, and C. D. Stinespring, Appl. Phys. Lett. **74**, 3836 (1999).

[20]E. Iliopoulos, A. Adikimenakis, E. Dimakis, K. Tsagaraki, G. Konstantinidis, and A. Georgakilas, "Active nitrogen species dependence on radiofrequency plasma source operating parameters and their role in GaN growth," J. Cryst. Growth **278**, 426–430 (2005).
[21]T. Kikuchi, A. S. Somintac, O. Ariyada, M. Wada, and T. Ohachi, J. Cryst. Growth **292**, 221 (2006).
[22]H. Carrère, A. Arnoult, E. Bedel-Pereira, and A. Ricard, J. Vac. Sci. Technol., B **22**, 2448 (2004).
[23]S. Agarwal, B. Hoex, M. Sanden, D. Maroudas, and E. S. Aydil, "Absolute densities of N and excited N_2 in a N_2 plasma," Appl. Phys. Lett. **83**, 4918 (2003).
[24]T. H. Meyers, M. R. Millecchia, A. J. Ptak, K. S. Zeimer, and C. D. Stinespring, "Influence of active nitrogen species on high temperature limitations for (0001_) GaN growth by rf plasma-assisted molecular beam epitaxy," J. Vac. Sci. Technol., B **17**, 1654 (1999).
[25]T. Czerwiec, F. Greer, and D. B. Graves, "Nitrogen dissociation in a low pressure cylindrical ICP discharge studied by actinometry and mass spectrometry," J. Phys. D: Appl. Phys. **38**, 4278 (2005).
[26]R. P. Vaudo, J. W. Cook, Jr., and F. Schetzina, "Atomic nitrogen production in a molecular-beam epitaxy compatible electron cyclotron resonance plasma source," J. Vac. Sci. Technol., B **12**, 1232 (1994).
[27]R. W. McCullough, J. Geddes, J. A. Croucher, J. M. Woolsey, D. P. Higgins, M. Schlapp, and H. B. Gilbody, "Atomic nitrogen production in a high efficiency microwave plasma source," J. Vac. Sci. Technol., A **14**, 152 (1996).
[28]D. Voulot, R. W. McCullough, R. Thompson, D. Burns, J. Geddes, G. J. Cosimini, E. Nelson, P. P. Chow, and J. Klassen, "Determination of the atomic nitrogen flux from a radio frequency plasma nitride source for molecular beam epitaxy systems," J. Vac. Sci. Technol., A **16**, 3434 (1998).
[29]S. H. Cho, H. Okumura, and K. Akimoto, "Comparison of excited nitrogen sources for molecular-beam-epitaxy GaN growth: Radio frequency and electron cyclotron resonance plasma sources," Appl. Phys. Lett. **76**, 3861 (2000).
[30]A. N. Wright and C. A. Winkler, *Active Nitrogen* (Academic Press, New York, 1968).
[31]A. Wierzbicka, Z. R. Zytkiewicz, S. Kret, J. Borysiuk, P. Dluzewski, M. Sobanska, K. Klosek, A. Reszka, G. Tchutchulashvili, A. Cabaj, and E. Lusakowska, "Influence of substrate nitridation temperature on epitaxial alignment of GaN nanowires to Si(111) substrate," Nanotechnology **24**, 035703 (2013).
[32]P. Kumar, M. Tuteja, M. Kesaria, U. V. Waghmare, and S. M. Shivaprasad, "Superstructure of self-aligned hexagonal GaN nanorods formed on nitride Si (111) surface," Appl. Phys. Lett. **101**, 131605 (2012).
[33]L. Geelhaar, C. Ch'eze, B. Jenichen, O. Brandt, C. Pfuller, S. Münch, R. Rothemund, S. Reitzenstein, A. Forchel, T. Kehagias, P. Komninou, G. P. Dimitrakopulos, T. Karakostas, L. Lari, P. R. Chalker, M. H. Gass, and H. Riechert, "Properties of GaN nanowires grown by molecular beam epitaxy," IEEE J. Sel. Top. Quantum Electron. **17**, 878 (2011).
[34]V. Consonni, M. Knelangen, A. Trampert, L. Geelhaar, and H. Riechert, "Nucleation and coalescence effects on the density of self-induced GaN nanowires grown by molecular beam epitaxy," Appl. Phys. Lett. **98**, 071913 (2011).